Memorias del 2022 Congreso Nacional de Control Automático
12-14 de Octubre, 2022. Tuxtla Gutiérrez, México.

Adaptive Integral Terminal Sliding Mode Guidance and Control for a UUV Under Perturbations

Andres E. Sanchez-Calvo * **V. Sebastian Martinez-Perez** *
Alejandro Gonzalez-Garcia * **Herman Castañeda** *

* *Tecnologico de Monterrey, School of Science and Engineering, Av. Eugenio Garza Sada 2501 Sur, 64849 Monterrey, N.L., Mexico. (e-mail: a01351370@tec.mx, a01232474@tec.mx, a00818249@tec.mx, hermancc@tec.mx).*

Abstract: This article addresses robust guidance and control for a fully-actuated underwater autonomous vehicle under external perturbations. A cascade strategy based on an adaptive integral terminal sliding mode controller is designed. Such approach ensures practical finite-time convergence of the tracking errors and robustness against disturbances with unknown boundaries. In addition, it does not overestimate the control gain, reducing chattering. The guidance law forces the vehicle to track desired trajectories, providing velocity and heading references for all degrees of freedom. Then, a low-level control ensures convergence of all the state variables. Finally, simulations results carried on a full model subject to water currents prove the feasibility and advantages of the proposed control scheme.

Keywords: Unmanned underwater vehicles, Guidance-Control, finite-time convergence, adaptive integral terminal sliding mode control, robust control.

1. INTRODUCTION

Over the past years, there has been a growing demand for UUVs (Unmanned Underwater Vehicle) due to the rise of scientific and industrial interest He et al. (2020), as these crafts can operate in hazardous environments and are a low-cost alternative to perform underwater activities. Moreover, UUVs have the potential to increase their presence in a wide range of applications such as surveillance, offshore exploration, aquaculture, military missions, archaeology, and maintenance of sub-aquatic infrastructure. Furthermore, a UUV is a self-propelled submersible which can be fully autonomous, equipped with its own energy supply, thrust, navigation, and control systems Christ and Wernli (2014).

To achieve fully autonomous behavior, trajectory tracking is a motion control problem that should be considered. In such problem, the system is forced to track a time-parameterized reference. However, it is challenging to implement a reliable trajectory tracking, since UUVs are affected by the highly nonlinear dynamics, uncertainties of model parameters, and external disturbances due to the underwater environment, like water currents. Hence, robust control methods are well suited solutions that focus on attaining system reliability under non optimal circumstances Zhang (2010).

To cope with the UUV tracking problem, different controllers have been proposed. For instance, Ali et al. (2021) proposed a twin controller approach, which is composed of a Proportional Integral Derivative (PID) controller along with a Model Reference Adaptive Control (MRAC) that minimizes the system disturbances. A hybrid technique based on fuzzy PID, and dynamic compensation was developed in Dong et al. (2020), to perform depth control. The use of neural networks to approximate unknown nonlinear functions of the model along a sliding mode controller was investigated in Guo et al. (2019) to accomplish target tracking tasks.

A widely used control technique which provides robustness against unmodeled dynamics and insensitivity to perturbations is the Sliding Mode Control (SMC), which establishes a variable structure that switches from one to another member of a set of possible values (Utkin, 1977). Hence, the system moves towards the sliding surface and stays at it. Consequently, a number of SMC variants have been employed to deal with UUV trajectory tracking issues. In Kim et al. (2021), a SMC along a sliding perturbation observer is applied to underwater vehicles.

Nevertheless, the SMC technique produces chattering effect that causes instability and irregular motions. Thus, it is important to reduce the chattering effect, as it can generate not feasible control signals or even cause actuator damage. To deal with it, there are several techniques that mitigates the chattering. For instance, a High Order Sliding Mode Controller like the super-twisting method is adopted in Ismail and Putranti (2015), where the chattering effect is theoretically eliminated and robust tracking of the UUV is achieved. On the other hand, Adaptive Sliding Mode Controller (ASMC) is another effective technique that minimizes chattering thanks to an

adaptive gain, which changes its value depending on the needed control effort to suppress disturbances, therefore the control gain is not overestimated Gonzalez-Garcia and Castaneda (2021). In Huang et al. (2008) an ASMC approach for nonlinear systems with uncertain parameters guarantees tracking performance. The design of a ASMC to control surge speed and heading of a USV subject to perturbations was investigated in Gonzalez-Garcia and Castaneda (2021). Lastly, an ASMC attitude controller for underwater vehicles was designed and implemented in Cui et al. (2016), where a nonlinear disturbance observer was included in the control scheme to compensate internal and external uncertainties.

However, the aforementioned SMC and ASMC techniques are based on a linear sliding surface, which guarantee asymptotic error convergence, whereas Terminal Sliding Mode Controller (TSMC) is a robust technique whose nonlinear sliding surface was designed to reach finite-time equilibrium, improve the transient response, and assure control accuracy. The principle of the TSMC sliding surface is the terminal attractor that was introduced in Zak (1989) with a neural learning application, later it was employed to motion control systems in Venkataraman and Gulati (1993). Therefore, this control strategy has been the root to develop various vehicle control systems. For example, in Elmokadem et al. (2017) a TSMC scheme was proposed to perform the lateral motion of an underactuated underwater vehicle. Then, in Ghadiri et al. (2021) an Adaptive Super-Twisting Non-Singular TSMC was investigated to decrease control signal chattering of a quadrotor. Nonetheless, TSMC has a singularity concern that stresses the system and generates complex numbers. Then, Integral TSMC is a method whose purpose is to avoid the singularity concern as well as to achieve finite-time equilibrium. The ITSMC sliding surface is a first order function that forces the system to begin inside the surface whenever the error initial values of $e(0)$ are known. In Wu et al. (2021) a Non-Singular ITSMC is addressed for a 5-DOF underwater vehicle to solve the trajectory tracking problem.

The contribution of this article is the design of a robust controller for a fully-actuated unmanned underwater vehicle subject to water currents and model parameters uncertainty. A cascaded strategy is adopted in order to deal with two first order subsystems, which are based on Adaptive Integral Terminal Sliding Mode Control (AITSMC) for trajectory tracking of UUVs. Such method provides finite-time tracking error convergence, eliminates the reaching phase and assures control accuracy. Meanwhile, the adaptive control gain avoids overestimated gains, mitigates the chattering effect, and maintains robustness against external perturbations with unknown boundaries. Under such properties, a guidance law is designed following the AITSMC strategy which provides the desired velocity references to the control law, which is formulated on the such algorithm. Finally, numerical simulations results demonstrate the UUV capability to track the desired trajectories in presence of water currents, exhibiting robustness and accuracy of the proposed control scheme.

The paper is organized as follows: Section 2 presents the dynamic model of the UUV and perturbations. Section 3 addresses the design of the controller and guidance law. In Section 4, the simulation results are illustrated. Finally, conclusions are drawn.

2. UUV MODEL

In this section, the VTec U-IV UUV dynamic model, vehicle parameters and a description of the water current disturbances are addressed. Fig. 1 shows the UUV prototype utilized to develop the proposed control scheme. On the other hand, Fig. 2 displays the inertial and body-fixed reference frame diagram of the UUV.

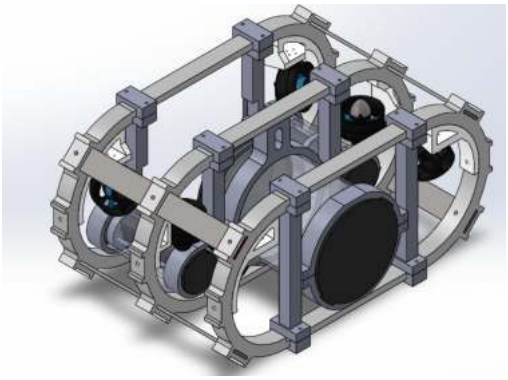

Fig. 1. VTec U-IV UUV CAD Prototype

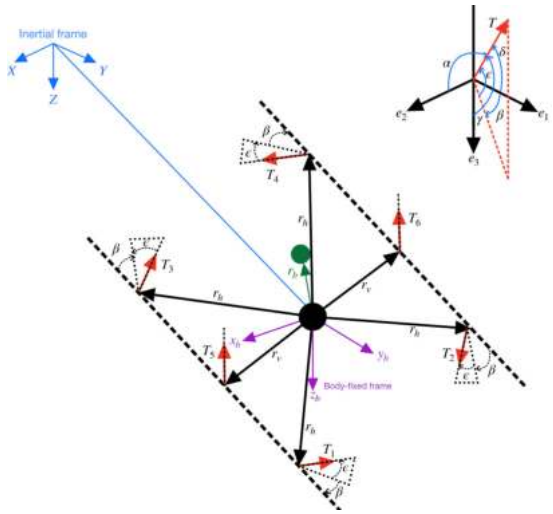

Fig. 2. VTec U-IV UUV reference frames, and at top right corner includes thurster configuration

2.1 UUV mathematical model

The 6 DOF marine craft equations (Fossen, 2011) of motion are expressed by:

$$\boldsymbol{M}\dot{\boldsymbol{\nu}} + \boldsymbol{C}(\boldsymbol{\nu})\boldsymbol{\nu} + \boldsymbol{D}(\boldsymbol{\nu})\boldsymbol{\nu} + \boldsymbol{g}(\boldsymbol{\eta}) = \boldsymbol{\tau} \quad (1)$$

$$\dot{\boldsymbol{\eta}} = \boldsymbol{J}(\boldsymbol{\eta})\boldsymbol{\nu} \quad (2)$$

where $\boldsymbol{\eta}$ and $\boldsymbol{\nu}$ are the position vector in the inertial frame $\boldsymbol{\eta} = [x, y, z, \phi, \theta, \psi]^T$, and the velocity vector in the body-fixed frame $\boldsymbol{\nu} = [u, v, w, p, q, r]^T$, respectively. In addition,

$\boldsymbol{M} = \boldsymbol{M}_{RB} + \boldsymbol{M}_A$ is composed of a rigid body and added mass matrix, which represents the craft inertia as follows:

$$\boldsymbol{M}_{RB} = \text{diag}[m, m, m, I_{xx}, I_{yy}, I_{zz}] \tag{3}$$

$$\boldsymbol{M}_A = \text{diag}[X_{\dot{u}}, Y_{\dot{v}}, Z_{\dot{\omega}}, K_{\dot{p}}, M_{\dot{q}}, N_{\dot{r}}] \tag{4}$$

$\boldsymbol{C}(\boldsymbol{v}) = \boldsymbol{C}_{RB} + \boldsymbol{C}_A$ consider the Coriolis and centripetal effect, due to the rotation of the body-fixed frame about the inertial frame. It is composed by a rigid body matrix $\boldsymbol{C}_{RB}$, and an added mass matrix $\boldsymbol{C}_A$,

$$\boldsymbol{C}_{RB}(\boldsymbol{v}) = \begin{bmatrix} \boldsymbol{0}_{3x3} & -m\boldsymbol{S}(\boldsymbol{v}_{lin}) \\ -m\boldsymbol{S}(\boldsymbol{v}_{lin}) & -\boldsymbol{S}(\boldsymbol{I}_g \boldsymbol{v}_{rot}) \end{bmatrix} \tag{5}$$

$$\boldsymbol{C}_A(\boldsymbol{v}) = \begin{bmatrix} 0 & 0 & 0 & 0 & -Z_{\dot{\omega}}\omega & Y_{\dot{v}}v \\ 0 & 0 & 0 & Z_{\dot{\omega}}\omega & 0 & -X_{\dot{u}}u \\ 0 & 0 & 0 & -Y_{\dot{v}}v & X_{\dot{u}}u & 0 \\ 0 & -Z_{\dot{\omega}}\omega & Y_{\dot{v}}v & 0 & -N_{\dot{r}}r & M_{\dot{q}}q \\ Z_{\dot{\omega}}\omega & 0 & -X_{\dot{u}}u & N_{\dot{r}}r & 0 & -K_{\dot{p}}p \\ -Y_{\dot{v}}v & X_{\dot{u}}u & 0 & -M_{\dot{q}}q & K_{\dot{p}}p & 0 \end{bmatrix} \tag{6}$$

where m is the mass, $\boldsymbol{S}$ is a skew-symmetric matrix, $\boldsymbol{v}_{lin} = [u, v, w]^T$ is the linear velocity vector, $\boldsymbol{v}_{rot} = [p, q, r]^T$ is the angular velocity vector and $\boldsymbol{I}_g = diag[I_{xx}, I_{yy}, I_{zz}]$ is the inertia. Restoring forces vector $\boldsymbol{g}(\boldsymbol{\eta})$ depend on the vehicle orientation, that yields equation (7)

$$\boldsymbol{g}(\boldsymbol{\eta}) = \begin{bmatrix} (W-B)s\theta \\ -(W-B)c\theta s\phi \\ -(W-B)c\theta c\phi \\ -r_{b,z}Bc\theta s\phi \\ -r_{b,z}Bs\theta \\ 0 \end{bmatrix} \tag{7}$$

where W is the weight of the craft and B is the buoyancy force of the vehicle.

The damping matrix $\boldsymbol{D}(\boldsymbol{v})$ are forces related to the velocity of the UUV, it is composed of a linear part that considers linear skin friction and a nonlinear part which contains higher order terms such as turbulent friction and vortexes.

$$\begin{aligned} \boldsymbol{D}(\boldsymbol{v}) = &-\text{diag}[X_u, Y_v, Z_w, K_p, M_q, N_r] \\ &-\text{diag}[X_{u|u|}|u|, Y_{|v|v}|v|, Z_{|w|w}|w|, K_{|p|p}|p|, M_{|q|q}|q|, N_{|r|r}|r|] \end{aligned} \tag{8}$$

Additionally, $\boldsymbol{\tau} = [X, Y, Z, K, M, N]^T$ is a vector of forces and moments produced by the six thrusters of VTec U-IV UUV. Furthermore, equation (2) contains the six degrees of freedom kinematic equations, where $\boldsymbol{J}(\boldsymbol{\eta})$ is defined as following.

$$\boldsymbol{J}(\boldsymbol{\eta}) = \begin{bmatrix} \boldsymbol{R}(\boldsymbol{\eta}) & \boldsymbol{0}_{3x3} \\ \boldsymbol{0}_{3x3} & \boldsymbol{T}(\boldsymbol{\eta}) \end{bmatrix} \tag{9}$$

$$\boldsymbol{R}(\boldsymbol{\eta}) = \begin{bmatrix} c\psi c\theta & -s\psi c\phi + c\psi s\theta s\phi & s\psi s\phi + c\psi c\phi s\theta \\ s\psi c\theta & c\psi c\phi + s\phi s\theta s\psi & -c\psi s\phi + s\theta s\psi c\phi \\ -s\theta & c\theta s\phi & c\theta c\phi \end{bmatrix}$$

$$\boldsymbol{T}(\boldsymbol{\eta}) = \begin{bmatrix} 1 & s\phi t\theta & c\phi t\theta \\ 0 & c\phi & -s\phi \\ 0 & s\phi/c\theta & c\phi/c\theta \end{bmatrix}$$

2.2 Vehicle parameters

The UUV consists of a front facing oval with a quasi-rectangular shape that encompasses three cylindrical enclosures that stores the hardware. Moreover, the UUV is 0.5% positively buoyant with respect to the vehicle weight.

Table 1. VTec U-IV parameters

Parameter	Value	Parameter	Value
Length	0.48 [m]	I_{yy}	1.75 $[kg/m^2]$
Height	0.36 [m]	I_{zz}	1.43 $[kg/m^2]$
Beam	0.72 [m]	$X_{\dot{u}}$	16.8374
Mass [m]	24 [kg]	$Y_{\dot{v}}$	20.2748
Volume	0.0252 $[m^3]$	$Z_{\dot{w}}$	35.3180
Weight (W)	234.44 [N]	$K_{\dot{p}}$	0.2165
Buoyancy (B)	245 [N]	$M_{\dot{q}}$	0.6869
β	20 [deg]	$N_{\dot{r}}$	0.6157
ε	15 [deg]	X_u	-0.3431
α	75.92 [deg]	Y_v	0.0518
δ	24.81 [deg]	Z_w	-0.5841
γ	105 [deg]	K_p	0.0064
$r_{b,z}$	-0.10726 [m]	M_q	0.04
$r_{h,x}$	0.1867 [m]	N_r	-0.1063
$r_{h,y}$	0.2347 [m]	$X_{\|u\|u}$	-111.7397
$r_{h,z}$	0.0175 [m]	$Y_{\|v\|v}$	-44.4058
$r_{v,x}$	0 [m]	$Z_{\|\omega\|\omega}$	-157.1951
$r_{v,y}$	0.2384 [m]	$K_{\|p\|p}$	-0.4634
$r_{v,z}$	0 [m]	$M_{\|q\|q}$	-0.2902
I_{xx}	0.9 $[kg/m^2]$	$N_{\|r\|r}$	-2.2897

The vehicle parameters were calculated using strip theory and computational fluid dynamic methodologies Eidsvik (2015). In Table 1 physical parameters of VTec U-IV UUV are presented.

2.3 Thruster configuration

Since, a costumize UUV is considered, generalized control forces $\boldsymbol{\tau} \in R^n$ needs to be distributed to the actuators in terms of control inputs. Hence, a torque vector is defined considering VTec U-IV thrust vector as well as the mapping matrix of the thruster configuration, which yields vector (10).

$$\boldsymbol{\tau} = \begin{bmatrix} (T_1 + T_2 - T_3 - T_4)|c\delta| \\ (-T_1 + T_2 - T_3 + T_4)|s\alpha| \\ -(T_5 + T_6) + (-T_1 - T_2 + T_3 + T_4)c\gamma \\ (-T_1 + T_2)\rho_1 + (T_3 - T_4)\rho_2 + (-T_5 + T_6)r_{v_y} \\ (T_1 + T_2)\rho_3 + (T_3 + T_4)\rho_4 \\ (-T_1 + T_2 + T_3 - T_4)\rho_5 \end{bmatrix} \tag{10}$$

where $\rho_1 = (r_{hy}|c\gamma| + r_{hz}|c\alpha)|$, $\rho_2 = (r_{hy}|c\gamma| - r_{hz}|c\alpha|)$, $\rho_3 = (r_{hx}|c\gamma| - r_{hz}|c\delta|)$, $\rho_4 = (r_{hx}|c\gamma| + r_{hz}|c\delta|)$ and $\rho_5 = (r_{hx}|c\alpha| + r_{hy}|c\delta|)$. Furthermore, it is important to notice that the thrusters have been tilted with an angle ϵ and a direction β. Therefore, the prior configuration enables fully-actuation and prioritize longitudinal movement. In addition, the thruster positions are defined by vectors; $||\boldsymbol{r}_{h,1}|| = ||\boldsymbol{r}_{h,2}|| = ||\boldsymbol{r}_{h,3}|| = ||\boldsymbol{r}_{h,4}|| = \sqrt{{r_{h,x}}^2 + {r_{h,y}}^2 + {r_{h,z}}^2}$ and $||\boldsymbol{r}_{v,1}|| = ||\boldsymbol{r}_{v,2}|| = \sqrt{{r_{v,x}}^2 + {r_{v,y}}^2 + {r_{v,z}}^2}$. Previous mentioned parameters $\epsilon, \beta, \boldsymbol{r}_h$ and $\boldsymbol{r}_v$ can be found in Table 1.

2.4 External disturbances

A UUV is mainly exposed to water currents, which are circulation systems of ocean waters. To consider the

ocean currents effect into the UUV dynamical model the following equation is applied (Fossen, 2011):

$$\boldsymbol{M}\dot{\boldsymbol{v}} + \boldsymbol{C}_{RB}(\boldsymbol{v})\boldsymbol{v} + \boldsymbol{C}_A(\boldsymbol{v}_r)\boldsymbol{v}_r + \boldsymbol{D}(\boldsymbol{v}_r)\boldsymbol{v}_r + \boldsymbol{g}(\boldsymbol{\eta}) = \boldsymbol{\tau} \quad (11)$$

where $\boldsymbol{v}_r = \boldsymbol{v} - \boldsymbol{v}_c$ is the relative velocity vector, and $\boldsymbol{v}_c$ is the current speed that is obtained following the Gauss-Markov process, that begins by solving the next first-order equation:

$$\dot{V}_c + \mu_c V_c = \omega_c \quad (12)$$

V_c is the speed magnitude, $\mu > 0$ is a constant and w is a Gaussian white noise. Then, for a 3-D irrotational water current the next expression is given:

$$\boldsymbol{v^n}_c = \begin{bmatrix} V_c c(\alpha_c)c(\beta_c) \\ V_c s(\beta_c) \\ V_c s(\alpha_c)c(\beta_c) \\ 0 \\ 0 \\ 0 \end{bmatrix} \quad (13)$$

where α_c and β_c are the attack and sideslip angle, respectively. Also, $\boldsymbol{v^n}_c$ is the current velocity vector in the inertial frame, so it should be rotated to get the current velocity in the body-fixed frame.

3. GUIDANCE AND CONTROL DESIGN

In this section, a cascaded control is designed, where a guidance law provides velocity references to the low-level controller. Hence, the control objective is to force the system state x to track the desired trajectories x_d in presence of water currents and unmodeled parameters. Then, an integral sliding surface is considered as follows:

$$s = e + \alpha e_I \quad (14)$$

$$\dot{e}_I = sign(e)|e|^{\beta} \quad (15)$$

where $\alpha > 0$ and $0 < \beta < 1$ are constant values, and since $e_I(0) = -e(0)/\alpha$, implies that the system starts in the sliding mode.

3.1 Guidance law

The guidance law based on adaptive integral sliding mode control is addressed. The first step is to define the pose error, given by:

$$\boldsymbol{e}_\eta(t) = \boldsymbol{\eta}_d - \boldsymbol{\eta} \quad (16)$$

where $\boldsymbol{e}_\eta(t)$ represents the position error in the inertial reference frame. Then, let represent us the system in the state space form given by:

$$\dot{\boldsymbol{x}}_1 = \boldsymbol{f}_1(\boldsymbol{x}_1) + \boldsymbol{g}_1(\boldsymbol{x}_1)\boldsymbol{u}_1 \quad (17)$$

where $\dot{\boldsymbol{x}}_1 = \dot{\boldsymbol{\eta}}$ is the velocity vector in the inertial reference frame, $\boldsymbol{f}_1(\boldsymbol{x}_1) = 0_{6x1}$ as the guidance law does not consider any hydrodynamic element, $\boldsymbol{g}_1(\boldsymbol{x}_1) = \boldsymbol{J}(\boldsymbol{\eta})$ is the transformation matrix and $\boldsymbol{u}_1 = \boldsymbol{v}_d$ provides the reference velocity to the control law.
To obtain the guidance law, (17) is substituted in the first derivative of the following sliding surface:

$$\dot{\boldsymbol{s}}_{\boldsymbol{\eta}} = \dot{\boldsymbol{x}}_{d1} - \dot{\boldsymbol{x}}_1 + \boldsymbol{\alpha}_\eta \dot{\boldsymbol{e}}_I \quad (18)$$

$$\dot{\boldsymbol{s}}_\eta = \dot{\boldsymbol{x}}_{d1} - \boldsymbol{g}(\boldsymbol{x}_1)\boldsymbol{u}_1 + \boldsymbol{\alpha}_\eta \dot{\boldsymbol{e}}_I \quad (19)$$

where, $\dot{\boldsymbol{x}}_{d1}$ contains the derivative of the reference positions from $\boldsymbol{\eta}_d$. Then, using feedback linearization method, it can be resolved for the control input $\boldsymbol{u}_1$ as:

$$\boldsymbol{u}_1 = \boldsymbol{g}(\boldsymbol{x}_1)^{-1}(\dot{\boldsymbol{x}}_{d1} + \boldsymbol{\alpha}_\eta \dot{\boldsymbol{e}}_I - \boldsymbol{u}_\eta) \quad (20)$$

where an auxiliary control $\boldsymbol{u}_\eta$ is added to provide robustness and denoted as follows:

$$u_{\eta,i} = -K_{1,i} sign(s_i)|s_i|^{\frac{1}{2}} - K_{2,i} s \quad (21)$$

where $i = [x, y, z, \phi, \theta, \psi]$ and $K_{1,i}$ is the adaptive gain, which is adjusted following the adaptation law presented in Gonzalez-Garcia and Castañeda (2021):

$$\dot{K}_{1,i} = \begin{cases} K_{\alpha,i} sign(|s_i| - \mu_i), & \text{if } K_{1,i} > K_{min,i} \\ K_{min,i} & \text{if } K_{1,i} \leq K_{min,i} \end{cases} \quad (22)$$

where $K_{\alpha,i}$ regulates the adaptive ratio, $K_{min,i}$ is the minimum value allowed for the adaptive gain, μ_i is a constant that detects the loss of the sliding surface and thus increases the gain. Additionally, $K_{2,i}$ helps the adaptive gain to reach the sliding surface.

3.2 Control law

The control law also based on an adaptive integral terminal sliding mode approach is adopted, producing the forces and moments $\boldsymbol{\tau}$ that the UUV needs to perform. The velocity error is defined as follows:

$$\boldsymbol{e}_v(t) = \boldsymbol{v}_d - \boldsymbol{v} \quad (23)$$

where $\boldsymbol{e}_v(t)$ denotes the velocity error in the body-fixed reference frame. The state space form of the system is represented as:

$$\dot{\boldsymbol{x}}_2 = \boldsymbol{f}_2(\boldsymbol{x}_2) + \boldsymbol{g}_2(\boldsymbol{x}_2)\boldsymbol{u}_2 \quad (24)$$

where $\dot{\boldsymbol{x}}_2 = \dot{\boldsymbol{v}}$ is the acceleration in the body-fixed reference frame, $\boldsymbol{f}_2(\boldsymbol{x}_2) = \boldsymbol{M}^{-1}(-\boldsymbol{C}(\boldsymbol{v})\boldsymbol{v} - \boldsymbol{D}(\boldsymbol{v})\boldsymbol{v} - \boldsymbol{g}(\boldsymbol{\eta}))$ contains the hydrodynamic elements of equation (1), $\boldsymbol{g}_2(\boldsymbol{x}_2) = \boldsymbol{M}^{-1}$ is the inverse of the mass matrix and $\boldsymbol{u}_2 = \boldsymbol{\tau}$ is the thrust vector.
To obtain the control input, the system (24) is substituted in the first derivative of the sliding surface.

$$\dot{\boldsymbol{s}}_v = \dot{\boldsymbol{x}}_{d2} - \dot{\boldsymbol{x}}_2 + \boldsymbol{\alpha}_v \dot{\boldsymbol{e}}_I \quad (25)$$

Also, using previous definitions the next equation is yielded:

$$\dot{\boldsymbol{s}}_v = \dot{\boldsymbol{x}}_{d2} - \boldsymbol{f}(\boldsymbol{x}_2) - \boldsymbol{g}(\boldsymbol{x}_2)\boldsymbol{u}_2 + \boldsymbol{\alpha}_v \dot{\boldsymbol{e}}_I \quad (26)$$

Then, by using feedback linearison method, it can be resolved for the control variable $\boldsymbol{u}_2$ as

$$\boldsymbol{u}_2 = \boldsymbol{g}(\boldsymbol{x}_2)^{-1}(\dot{\boldsymbol{x}}_{d2} - \boldsymbol{f}(\boldsymbol{x}_2) + \boldsymbol{\alpha}_v \dot{\boldsymbol{e}}_I - \boldsymbol{u}_v \quad (27)$$

where an adaptive integral terminal sliding mode control $\boldsymbol{u}_v$ is added, and expressed as:

$$u_{v,j} = -K_{1,j} sign(s_j)|s_j|^{\frac{1}{2}} - K_{2,j} s \quad (28)$$

where $j = [u, v, w, p, q, r]$ and $K_{1,j}$ is the adaptive gain, which is defined as the previous adaptation law (22). Finally, in order to illustrate the complete control strategy, the Fig. 3 is introduced, where clearly exhibits the guidance outer loop and the inner control loop.

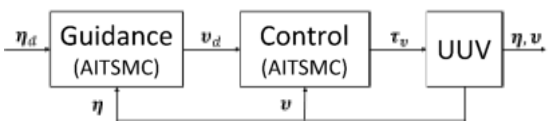

Fig. 3. Control-Guidance scheme

4. SIMULATION RESULTS

This section addresses the simulation results in order to verify the control performance and its robustness against external disturbances. The simulations were carried out in MATLAB Simulink, with a step time of 0.01 seconds solved by the Euler integration method.
A Dubin trajectory was given as reference to the system to test the AITSM controler in different scenarios. To prove the controller feasibility to follow different changes in direction, the desired trajectory consists of a combination of vertical, horizontal and curved lines. Such desired trajectory is defined as follows:

$$x_d(t) = \begin{cases} 0 \text{ m}, 0 \leq t < 20\text{s} \\ 0.2(t-20) \text{ m}, 20 \leq t < 40\text{s} \\ \sin(0.05\pi(t-40)) + 4 \text{ m}, 40 \leq t < 60\text{s} \\ -0.2(t-60) + 4 \text{ m}, 60 \leq t < 80\text{s} \\ -\sin(0.05\pi(t-80)) \text{ m}, 80 \leq t < 100\text{s} \\ 0.2(t-100) \text{ m}, 100 \leq t < 120\text{s} \end{cases} \tag{29}$$

$$y_d(t) = \begin{cases} 1 \text{ m}, 0 \leq t < 20s \\ 1 \text{ m}, 20 \leq t < 40s \\ -\cos(0.05\pi(t-40)) + 2 \text{ m}, 40 \leq t < 60s \\ 3 \text{ m}, 60 \leq t < 80s \\ -cos(0.05\pi(t-80)) + 4 \text{ m}, 80 \leq t < 100s \\ 5 \text{ m}, 100 \leq t < 120s \end{cases} \tag{30}$$

$$z_d(t) = \begin{cases} 0.2t + 1 \text{ m}, 0 <\leq t < 20 \\ 5 \text{ m}, 20 \leq t < 120s \end{cases} \tag{31}$$

$$(\phi_d, \theta_d, \psi_d)(t) = \{0 \text{ rad}, 0 \leq t < 120s \tag{32}$$

The controller assumes that the full state is always available by estimation or measurement. Furthermore, it is expected to use a IMU, a barometer and a DVL to obtain the state of the craft in the physical implementation. Also, as mentioned in Section 2, water currents were mathematically modeled as perturbations, where $\mu_c = 0.02$, w is a Gaussian noise at $100Hz$, $\alpha = 20°$ is the angle of attack and $\beta_c = 0°$ is the side slip angle, hence the disturbance has a constant direction. The previous values yield a pick of $50N$ as the highest disturbance force. Additionally, the initial state of the UUV is [x,y,z,ϕ,θ,ψ]=0.
Moreover, the applied disturbance is present during all the simulation time. Results are presented below:

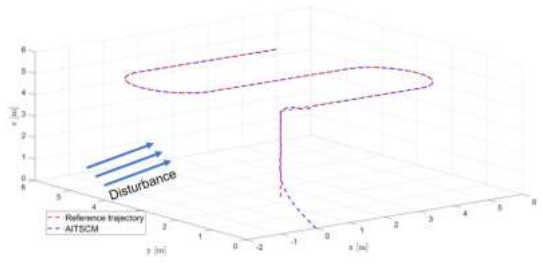

Fig. 4. 3D Dubin trajectory versus UUV response

In Fig. 4, the performance and accuracy of the UUV to follow the desired Dubin trajectory is exhibited. Furthermore, due to the changing trajectory some peaks can

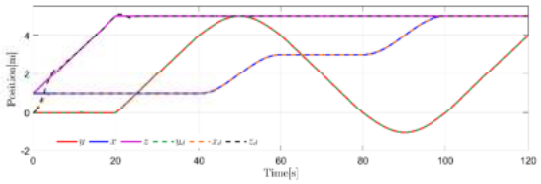

Fig. 5. Linear position responses

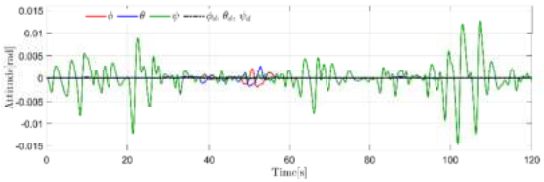

Fig. 6. Attitude responses

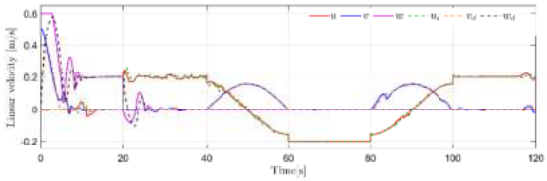

Fig. 7. Linear velocities of the UUV

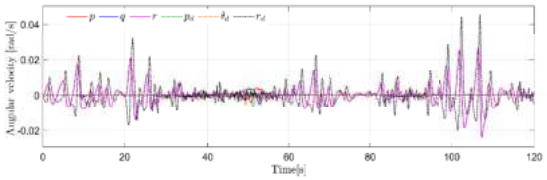

Fig. 8. Angular velocities of the UUV

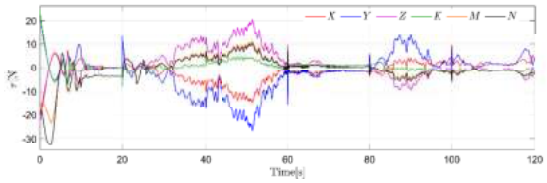

Fig. 9. Control input signals

be observed in the linear and angular responses. In Fig. 5 the system demonstrates its robustness against water currents, also it follows the desired trajectory as the state responses do not present deviations. Similarly, in Fig. 6, the attitude response is robust against disturbances as well, where the deviations are small enough such that the affectation to the UUV performance is minimal. Additionally, previous figures showcase the elimination of the reaching phase, which is a characteristic of the integral TSMC sliding surface that provides a faster convergence. Fig. 7 and 8 display the desired velocities provided by the guidance law, which have negligible oscillations that are a consequence of the perturbations. Moreover, the output signals prove the control law effectiveness at following the time-varying reference signals. Fig. 9 indicates that the trajectory is feasible to the physical capabilities of the UUV, as there is no saturation. Additionally, no

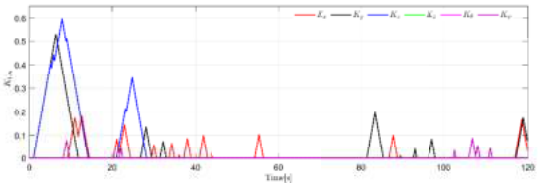

Fig. 10. Adaptive gains relative to the Guidance

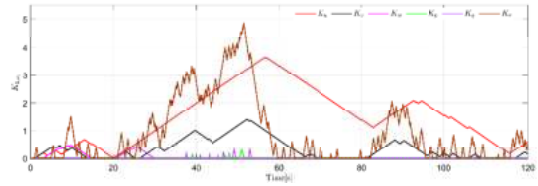

Fig. 11. Adaptive gains of the Control

chattering is presented, which is another advantage of the AITSMC that deals with unmodeled dynamics, consequently the system is not stressed. Last Figs. 10 and 11 are the gains which are constantly active to counter disturbances.

5. CONCLUSION

A robust control and guidance for an unmanned underwater vehicle subject to perturbations and model parameter uncertainty has been addressed. A cascaded control loop was proposed to handle the trajectory tracking problem, where the goal was to follow a Dubin reference. The guidance and control law were based on an adaptive integral terminal sliding mode control, such approach guarantees finite-time convergence, increases the system effectiveness and removes the sliding surface reaching phase. Moreover, water currents were modeled as disturbances and added to the simulation tests. Results showcased the robustness and accuracy of the proposed controller. Finally, tracking error finite-time convergence was achieved without any presence of saturation or chattering in the control signal.

6. ACKNOWLEDGEMENTS

This work was supported by the student group VantTec, as well as the VantTec sponsors: Techmake, SBG Systems, Google, IFM Efector, RoboNation, Velodyne LiDAR, NVIDIA, Akky, ZF Group, Güntner, and Siemens. Finally, the authors acknowledge the support from the university, Tecnologico de Monterrey, and the Robotics Laboratory of the Northeast and Central Mexico area.

REFERENCES

Ali, Z., Li, X., and Noman, M. (2021). Stabilizing the dynamic behavior and position control of a remotely operated underwater vehicle. *Wireless Personal Communications*, 116(2), 1293–1309.

Christ, R. and Wernli, R. (2014). *The ROV Manual: A User Guide for Remotely Operated Vehicles*. Elsevier, 2 edition.

Cui, R., Zhang, X., and Cui, D. (2016). Adaptive sliding-mode attitude control for autonomous underwater vehicles with input nonlinearities. *Ocean Engineering*, 123, 45–54.

Dong, M., Li, J., and Chou, W. (2020). Depth control of rov in nuclear power plant based on fuzzy pid and dynamics compensation. *Microsystem Technologies*, 26(3), 811–821.

Eidsvik, O. (2015). *Identification of Hydrodynamic parameters for ROVs*. Master's thesis, Norwegian Institute of Science and Technology.

Elmokadem, T., Zribi, M., and Youcef-Toumi, K. (2017). Terminal sliding mode control for the trajectory tracking of underactuated autonomous underwater vehicles. *Ocean Engineering*, 129, 613–625.

Fossen, T.I. (2011). *Handbook of Marine Craft Hydrodynamics and Motion Control*. John Wiley & Sons.

Ghadiri, H., Emami, M., and Khodadadi, H. (2021). Adaptive super-twisting non-singular terminal sliding mode control for tracking of quadrotor with bounded disturbances. *Aerospace Science and Technology*, 112.

Gonzalez-Garcia, A. and Castaneda, H. (2021). Guidance and control based on adaptive sliding mode strategy for a usv subject to uncertainties. *IEEE Journal of Oceanic Engineering*, 46(4), 1144–1154.

Gonzalez-Garcia, A. and Castañeda, H. (2021). Adaptive integral terminal sliding mode control for an unmanned surface vehicle against external disturbances. volume 54, 202–207.

Guo, Y., Qin, H., Xu, B., Han, Y., Fan, Q.Y., and Zhang, P. (2019). Composite learning adaptive sliding mode control for auv target tracking. *Neurocomputing*, 351, 180–186.

He, Y., Wang, D., and Ali, Z. (2020). A review of different designs and control models of remotely operated underwater vehicle. *Measurement and Control (United Kingdom)*, 53(9-10), 1561–1570.

Huang, Y.J., Kuo, T.C., and Chang, S.H. (2008). Adaptive sliding-mode control for nonlinear systems with uncertain parameters. *IEEE Transactions on Systems, Man, and Cybernetics, Part B: Cybernetics*, 38(2), 534–539.

Ismail, Z. and Putranti, V. (2015). Second order sliding mode control scheme for an autonomous underwater vehicle with dynamic region concept. *Mathematical Problems in Engineering*, 2015.

Kim, H.H., Lee, M.C., Cho, H.J., Hwang, J.H., and Won, J.S. (2021). Smcspo-based robust control of auv in underwater environments including disturbances. *Applied Sciences (Switzerland)*, 11(22).

Utkin, V. (1977). Survey paper: Variable structure systems with sliding modes. *IEEE Transactions on Automatic Control*, 22(2), 212–222.

Venkataraman, S. and Gulati, S. (1993). Control of nonlinear systems using terminal sliding modes. *Journal of Dynamic Systems, Measurement and Control, Transactions of the ASME*, 115(3), 554–560.

Wu, Z., Peng, H., Hu, B., and Feng, X. (2021). Trajectory tracking of a novel underactuated auv via nonsingular integral terminal sliding mode control. *IEEE Access*, 9, 103407–103418.

Zak, M. (1989). Terminal attractors in neural networks. *Neural Networks*, 2(4), 259–274.

Zhang, P. (2010). Chapter 2 - industrial control engineering. In *Advanced Industrial Control Technology*, 41–70. William Andrew Publishing, Oxford.